Ferromagnetic Bonding: High Spin Copper Clusters ($^{n+1}Cu_n$; $n = 2-14$) Devoid of Electron Pairs but Possessing Strong Bonding†

Sam P. de Visser,‡ Devesh Kumar,§ Mark Danovich,§ Nir Nevo,§ David Danovich,§ Pankaz K. Sharma,§ Wei Wu,|| and Sason Shaik*,§

The Manchester Interdisciplinary Biocenter and the School of Chemical Engineering and Analytical Science, The University of Manchester, Sackville Street, PO Box 88, Manchester M60 1QD, U.K., Department of Organic Chemistry and the Lise Meitner-Minerva Center for Computational Quantum Chemistry, Hebrew University of Jerusalem, 91904 Jerusalem, Israel, and State Key Laboratory of Physical Chemistry of Solid Surfaces, Center for Theoretical Chemistry, and Department of Chemistry, Xiamen University, Xiamen 361005, P. R. China

Received: September 11, 2005; In Final Form: February 10, 2006

Density functional theoretic studies are performed for the high-spin copper clusters $^{n+1}Cu_n$ ($n = 2-14$), which are devoid of electron pairs shared between atoms, hence *no-pair clusters* (*J. Phys. Chem.* **1988**, *92*, 1352; *Isr. J. Chem.* **1993**, *33*, 455; *J. Am. Chem. Soc.* **1999**, *121*, 3165). Despite the lack of electron pairing, it is found that the bond dissociation energy per atom (BDE/*n*) is significant and converges (to within 1 kcal mol^{-1}), around a cluster size $^{11}Cu_{10}$, to a value of BDE/$n = 19$ kcal mol^{-1}. This is a very large bonding energy, much larger than has previously been obtained for no-pair clusters of lithium, BDE/$n = 12$ kcal mol^{-1}, or sodium clusters, BDE/$n = 3$ kcal mol^{-1}. This bonding, so-called ferromagnetic bonding (FM-bonding) is analyzed using a valence bond (VB) model (*J. Phys. Chem. A* **2002**, *106*, 4961; *Phys. Chem. Chem. Phys.* **2003**, *5*, 158). As such, FM-bonding in no-pair clusters is described as an ionic fluctuation, of the triplet pair, that spreads over all the close neighbors of a given atom in the clusters. Thus, if we refer to each triplet pair and its ionic fluctuations as a local FM-bond, we can regard the electronic structure of a given $^{n+1}M_n$ cluster as *a resonance hybrid of all the local FM-bonds between close neighbors*. The model shows how a weak interaction in the diatomic triplet molecule can become a remarkably strong binding force that binds together mono-valent atoms without even a single electron pair. This is achieved because the growing number of VB structures exerts a cumulative effect of stabilization that is maximized when the cluster has a compact structure with an optimal coordination number for the atoms.

1. Introduction

No-pair ferromagnetic bonding is the type of bonding that involves no electron pair bonds and occurs, for instance, in high-spin alkali metal clusters.[1−6] To appreciate the term "no-pair bonding", consider in Scheme 1a, the Li_2 case where the 2s atomic orbitals of the two lithium atoms form a set of bonding (2σ, i.e., σ_g) and antibonding ($2\sigma^*$, i.e., σ_u) orbitals. In the singlet ground state, the two electrons will occupy the bonding orbital to form a dimer having an electron pair with singlet spin. By contrast, in the triplet $^3\Sigma^+_u$ state where one electron resides in the bonding orbital and one in the antibonding orbital, the resulting dimer would be devoid of electron pairing (the bond order is formally zero). Indeed, the $2\sigma^1 2\sigma^{*1}$ triplet configuration, in Scheme 1a, is the purely covalent triplet $2s(1)^1 2s(2)^1$ configuration, in Scheme 1b, where each Li contains a single electron localized in the respective 2s orbital, and which is repulsive and should cause the dimer to dissociate. However, the triplet $^3\Sigma^+_u$ state of Li_2 is actually bound,[3] albeit weakly, and the same is true for the other no-pair alkali dimers, which form weakly bonded triplet $^3\Sigma^+_u$ states.[7−10]

SCHEME 1: (a) Orbital Mixing of the Pure 2s Atomic Orbitals in $^3Li_2$, Where the Symmetry Labels of 2σ and $2\sigma^*$ Are Indicated in Parentheses, and (b) the Equivalence between the $2\sigma^1\ 2\sigma^{*1}$ and $2s(1)^1 2s(2)^1$ Configuration Representations, Where 1 and 2 in Parentheses Are Atom Numbers

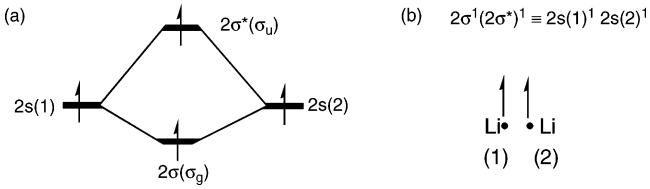

As was shown by means of high level calculations and valence bond (VB) theory,[3] the bonding arises due to the mixing in of higher lying structures into the ground-state wave function; an ionic structure, $^3(Li^+Li^-)$, in which the Li anion involves a $2s(1)^1 2p_z(1)^1$ configuration, and a covalent structure with a $2p_z(1)^1 2p_z(2)^1$ configuration, whereby the *z* axis is the Li- - -Li axis. Thus, while the configurations $2s(1)^1 2p_z(1)^1$ and $2p_z(1)^1 2p_z(2)^1$ are high lying, their mixing is sufficient to overcome the 2s−2s triplet repulsion and produce a shallow minimum.[3,5,11] As the cluster grows to $^{n+1}Li_n$ the number of

† Part of the "Chava Lifshitz Memorial Issue".

* To whom correspondence should be addressed. Telphone: +972-2-6585909. Fax: +972-2-6584680. E-mail: sason@yfaat.ch.huji.ac.il.

‡ The Manchester Interdisciplinary Biocenter and the School of Chemical Engineering and Analytical Science, The University of Manchester.

§ Department of Organic Chemistry and the Lise Meitner-Minerva Center for Computational Quantum Chemistry, Hebrew University of Jerusalem.

|| State Key Laboratory of Physical Chemistry of Solid Surfaces, Center for Theoretical Chemistry, and Department of Chemistry, Xiamen University.

10.1021/jp055125a CCC: $33.50
Published on Web 04/07/2006

high-spin ionic and excited covalent structures increases steeply, and so does the binding energy of the cluster, which grows and converges to 12 kcal mol^{-1} per atom, without even a single electron pair.[5] Henceforth, we refer to this type of bonding, *which occurs in maximum-spin clusters without electron pairs (no-pair clusters[2]), by the term ferromagnetic bonding (FM-bonding).* An alternative representation of FM-bonding was described by McAdon and Goddard,[1] using interstitial orbitals. The two representations are ultimately equivalent.[3,4]

These no-pair clusters are not merely theoretical curiosities for the purpose of demonstrating unusual bonding features; some of them have actually been made and probed by experimental techniques. Thus, laser-induced emission spectroscopy on the triplet lithium, sodium, potassium, rubidium and cesium dimers showed a weakly bound potential for the $^3\Sigma^+_u$ state.[7−9] In the case of sodium clusters, there exists spectroscopic evidence for the no-pair trimer species (^{4}A′), $^4Li_3$, $^4Na_3$, and $^4K_3$.[12−16] As such, these no-pair clusters are real entities, which enrich the scope of chemical bonding, and are therefore of wide general interest to chemists. An additional interest in this kind of clusters is their relationship to Bose−Einstein condensates (BECs) in which the quantum states of all atoms are identical, and to Fermi-"gases" of fermionic isotopes of alkali metals, (e.g., K with atomic mass 40) in magnetic fields.[16,17] Finally, the interest in magnetic clusters is intrinsically high for their potential applications in nanochemistry.

The present paper constitutes part of our ongoing program[3−6] to map the territory of these no-pair clusters in the periodic table. In previous studies we compared the FM-bonding in the no-pair clusters of sodium to those of lithium.[6] The sodium clusters, $^{n+1}Na_n$ ($n = 2-12$) were found to be much less strongly bound than the lithium clusters $^{n+1}Li_n$. Therefore, instead of continuing down the periodic table to potassium, we decided to search for strong FM-bonding among late transition metal analogues of the alkali atoms, namely, the column containing copper, silver and gold, which possess a closed-shell d-block and a singly occupied s-orbital.[18−20] Thus, electronically these systems are mono-valent analogues of the alkali metals and may therefore be prone to generate bound no-pair clusters with maximum spin. In fact, the $^3Cu_2$ dimer was spectroscopically probed in the $^3\Sigma^+_u$ state by Bondybey[21] who determined a bond-dissociation energy (BDE) of 1000−1500 cm^{-1} with an average bond length of 2.48 ± 0.03 Å. Since this bond energy is significantly stronger than the one in the corresponding $^3Li_2$ dimer, we decided to focus on the study $^{n+1}Cu_n$ no-pair clusters, with an attempt to find the structures and the maximum dissociation energy per atom, and then to model the bonding by a suitable VB model, as done before for the $^{n+1}Li_n$ no-pair clusters.[3,5]

2. Methods

The calculations presented here were performed with the Gaussian-98 and Gaussian-03 program packages, using a combination of different methods and basis sets.[22] We tested a few density functional methods, UB3LYP,[23,24] UB3P86,[23,25] and UB3PW91,[23,26] and the ab initio UCCSD(T) method for the copper dimer in the ground state and in the triplet $^3\Sigma^+_u$ state; these methods were benchmarked against available experimental BDE data for these states. Since the use of UCCSD(T) proved to be too time-consuming even for the dimer, we used DFT for all the higher clusters. The hybrid functionals gave good results, and UB3P86 was preferred as the choice method, for the sake of consistency with previous work.[4−6]

A few basis sets were tested to find the most suitable ones coupled with the different methods. Some of these basis sets included an effective core potential (ECP) on Cu, such as LANL2DZ with a relativistic ECP[27] and the 1997 Stuttgart relativistic small core ECP with extended valence basis set (with (8s7p6d)/[6s5p3d] contractions).[28] We also examined a few all-electron basis sets: Pople's 6-31G*, the Ahlrichs basis sets (pVDZ, TVZ and VTZ),[29] DGauss DZVP2 polarized DFT orbitals basis set, Wachters+f basis set,[30] and the augmented double-ζ atomic natural orbital (ANO) basis set of Roos et al.[31,32] The ECP/LANL2DZ, ECP/Stuttgart and ANO basis sets were found to give the most consistent results with different methods, and were therefore used throughout wherever possible.

In the case of the dimer, the $^3Cu_2$ no-pair state was the first excited state. In most cases, the no-pair state turned out to be among the lowest excited states. However, since there is no guarantee that the no-pair states will be the lowest excited state, for a given cluster, we routinely verified that in the state of choice the singly occupied orbital were only σ-types. The orbitals were examined in two ways: (a) Initially, using canonical Kohn−Sham (KS) orbitals, we made sure that no radial orbitals (perpendicular to the surface of the cluster) were singly occupied. (b) Subsequently, the singly occupied orbitals were localized, and the resulting orbitals were ascertained to be confined to a single atom and dominated by the 4s-type AO of Cu (see Supporting Information (SI) for the orbitals of $^5Cu_4$). In such a configuration, the $^{n+1}Cu_n$ species corresponds to the fundamental $s_1^1\ s_2^1 ... s_i^1, ..., s_n^1$ ($i = 1-n$, is the atomic index) no-pair electronic configuration mixed with some σ-type AOs. In addition, for every cluster the state was verified for stability of the DFT wave function, using the stability option in GAUSSIAN, as well as by means of TDDFT calculations that served to ascertain the lowest energy solution.

For each cluster size we tested different structures with different state symmetry, but our report here is restricted to the most stable clusters. More technical details are given in the Supporting Information (SI) to this paper. All calculations discussed here are the result of a full geometry optimization followed by tests for minima.

In the following sections, the term BDE stands for bond dissociation energy and BDE/n for bond dissociation energy per atom. Basis set superposition errors (BSSE) on the BDE and BDE/n values were tested using the counterpoise method (using the keyword Counterpoise = n [n is the number of Cu atoms in the cluster] in Gaussian-03).[22b]

Thus, each unique atom was calculated in the presence of the total basis set of the entire cluster, the energies were summed up and the sum gave the total energy of the dissociated atoms, corrected by BSSE. The energy difference of the dissociated atoms and the energy of the cluster gave, in turn, the BSSE corrected BDE. Since the clusters were of high symmetry (or with small deviation thereof), calculation of a single atom in the entire basis set, and multiplying the result by the number of atoms gave a very close estimate of the BSSE corrected energy of the dissociated atoms as well.

In the end of this procedure, we found the expected results: the large ANO basis set was found to exhibit negligible BSSE, whereas, the smaller LANL2DZ basis set exhibited significant BSSE. The ECP/Stuttgart basis set was found to have very small BSSE corrections comparable with the all electron ANO basis set. As discussed in the Results section, the BSSEs on the UB3P86/LANL2DZ BDE/n values were virtually constant for cluster sizes, $n = 5-14$. Furthermore, the BSSE corrected UB3P86/ANO and UB3P86/ECP/Stuttgart-based BDE/n values were very close to the uncorrected UB3P86/LANL2DZ values.

TABLE 1: Comparative Calculations of Bond Dissociation Energy (BDE), Interatomic Distance (r) and Frequency (ω) for $^1Cu_2$ Using Different Methods and Basis Sets[a,b]

	LANL2DZ			Ahlrichs p-VDZ			Wachters+f	
	BDE	r	ω	BDE	r	ω	BDE	r
UB3LYP	2.02	2.259	256.0	2.17	2.231	266.2	1.89	2.264
UB3P86	2.07	2.241	267.6	2.19	2.212	276.3	1.95	2.240
UB3PW91	1.93	2.253	260.5	2.04	2.223	270.6	1.82	2.252
UCCSD(T)	1.66	2.342	206.4	1.77	2.288	246.3	1.81	2.281

[a] The experimental data are BDE = 2.01 eV, r = 2.2197 Å and ω = 266.43 cm^{-1} (ref 19). [b] BDE in eV, r in Å, and ω in cm^{-1}.

TABLE 2: Comparative Calculations of Bond Dissociation Energy (BDE), Interactomic Distance (r) and Stretching Frequency (ω) of $^3Cu_2$ Using Different Methods and Basis Sets[a]

	BDE (eV)[b,c]	r (Å)	ω (cm^{-1})
UB3P86/6-311G*	0.643 (0.311)	2.531	
UCCSD(T)/6-311G*	0.000001	9.918	
	Ahlrichs Basis Sets		
UCCSD(T)/PVDZ	0.12 (−0.13)	2.641	
UB3P86/PVDZ	0.47 (0.16)	2.454	166.6
UCCSD(T)/TVZ	0.000 03	7.913	
UB3P86/TVZ	−0.05	2.835	31.0
UCCSD(T)/VTZ	0.000 03	7.884	
UB3P86/VTZ	0.037	2.606	108.6
UCCSD(T)/DZVP2[d]	0.127 (0.05)	3.052	50.10
UB3P86/DZVP2[d]	0.199 (0.10)	2.733	98.7
	Stuttgart/ECP-1997		
UCCSD(T)/ECP-1997[e]	0.065 (−0.01)	2.969	
UB3P86/ECP-1997[e]	0.132 (0.121)	2.607	104.6
	ANO Basis Set[f]		
UB3P86	0.132 (0.120)	2.629	
UB3LYP	0.050	2.703	
UCCSD(T)	0.019	3.097	
	LANL2DZ Basis Set		
UCCSD(T)	0.090 (−0.06)	3.039	50.1
UB3P86	0.238 (0.074)	2.614	105.6
	Experiment		
	0.15	2.48	125

[a] The experimental data is from ref 21. [b] In parentheses BDE with BSSE correction. [c] BDE($^3Li_2$) = 0.78 and 0.74 kcal mol^{-1} using BOVB/cc-pVDZ and BOVB/cc-pVTZ.[3,5] BDE($^3Na_2$) = 0.46 and 0.40 kcal mol^{-1} using B3P86/cc-pVDZ and B3P86/cc-pVTZ.[6] [d] Polarized DFT orbitals basis sets. [e] Stuttgart relativistic small core ECP basis set (1997). [f] Roos' augmented double-ζ atomic natural orbital basis.

3. Results

3.1. Bonding and Structure in No-Pair Clusters, $^{n+1}Cu_n$. The BDEs, bond lengths, and vibrational frequencies of the $^1Cu_2$ and $^3Cu_2$ species were initially studied using different computational levels (UB3LYP, UB3P86, UB3PW91, and UCCSD(T)) with various basis sets (LANL2DZ, ECP/Stuttgart, Ahlrichs-pVDZ, and Wachters+f, ANO, etc.), and the results were compared with experimental data.[19,21] The data are collected in Table 1 for the ground state, $^1Cu_2$, and in Table 2 for the $^3Cu_2$ state.

Inspection of Table 1 shows that, as noted by others,[33] here too, the UCCSD(T) method underestimates the bond dissociation energy and vibrational frequency of the copper dimers by 10−20%. Since the ground state is not in the focus of this study, we did not run extensive UCCSD(T) tests for the $^1Cu_2$ species, to ascertain it performance with larger basis sets. The DFT methods, in Table 1, gave reasonable agreement with the experimental data. Of the three tested basis sets, in Table 1, the Wachters+f basis set gave the poorest agreement with experiment.

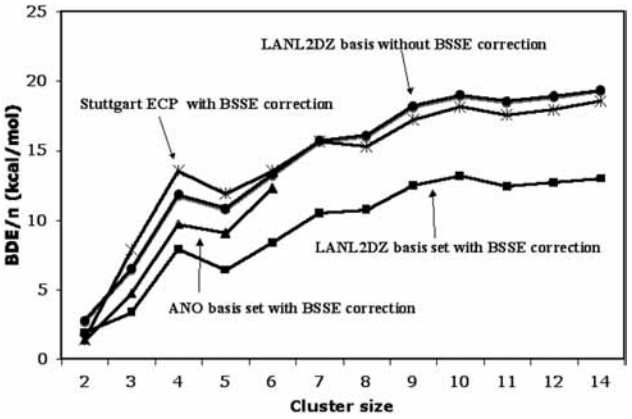

Figure 1. Plots of the BDE/n data vs n for $^{n+1}Cu_n$ (n = 2−14) using uncorrected UB3P86/LANL2DZ data; and BSSE corrected UB3P86/LANL2DZ, UB3P86/Stuttgart/ECP-1997, and UB3P86/ANO data.

The no-pair dimer, $^3Cu_2$, was more extensively studied and the results are collected in Table 2; results in parentheses are after BSSE correction. Here in addition to geometry optimization, and BDE determination, we performed also a full scan of the potential energy surface to ascertain that there is a single minimum deeper than the dissociation limit. Unfortunately, UCCSD(T) calculations considerably underestimated the BDE and give very long bond lengths in comparison with experiment. No attempt was made to further benchmark the UCCSD(T) method, since the UCCSD(T)/ANO geometry optimization calculation of the $^3Cu_2$ species was already extremely demanding and took 39 days of CPU time on a Pentium 3.2 GHz computer!

Generally, most of the calculations using the Ahlrichs basis sets gave unsatisfactory results with DFT or UCCSD(T) methods. By contrast, the hybrid DFT methods with the ANO, LANL2DZ, and StuttgartECP-1997 basis sets led to reasonable results for BDE but overestimated the equilibrium distance. As expected, the BSSE with ANO is very small (≤0.001 kcal/mol); it is also small for StuttgartECP-1997, but substantial with LANL2DZ. For the calculations of no-pair lithium clusters,[5] the UB3P86 method was found to be the most suitable. We therefore decided to select UB3P86 also for the $^{n+1}Cu_n$ clusters, for consistency with our previous work.

On the basis of the performance of the various basis sets, the choice levels for BDE calculations of no-pair clusters would have been UB3P86/ANO and/or StuttgartECP-1997. However, UB3P86/ANO calculations turned out to be too demanding beyond n = 6 (e.g., a counterpoise calculation on the cluster with n = 6 required 26 days of CPU time on a Pentium 3.2 GHz computer), and therefore, the ANO data is limited to n = 2−6. Thus, the entire study was conducted with UB3P86/LANL2DZ and UB3P86/StuttgartECP-1997 for all n values, while the results of UB3P86/ANO up to n = 6 served as benchmark values ("true" data) for the lower levels.

Different structures of the no-pair clusters, $^{n+1}Cu_n$ for n = 2−14, were tested, and the optimized structures are collected in the SI document. Table 3 collects all the BDE/n values for the most stable clusters with the LANL2DZ, StuttgartECP-1997, and ANO basis sets, while Figure 1 shows four plots of the BDE/n values as a function of the cluster size using the BSSE corrected ANO, StuttgartECP-1997 and LANL2DZ data, as well as the uncorrected LANL2DZ data. First, it is apparent that *all the plots exhibit the same pattern*. Second, starting with n = 4 onward, the corrected and uncorrected LANL2DZ plots are virtually parallel to one another, differing by almost a constant quantity. Finally, the ANO results wherever present, are close to the uncorrected LANL2DZ data; in particular for n = 6, the

TABLE 3: Bond Dissociation Energy Per Atom (BDE/*n*) Values for $^{n+1}Cu_n$ Clusters Calculated by UB3P86 Method with LANL2DZ, Stuttgart/ECP-1997, and ANO Basis Sets

cluster	LANL2DZ BDE/*n* without BSSE	LANL2DZ BDE/*n* with BSSE	Stuttgart BDE/*n* with BSSE	ANO BDE/*n* with BSSE
$^3Cu_2$	2.75	1.89	1.39	1.39
$^4Cu_3$	6.50	3.37	7.89	4.72
$^5Cu_4$	11.82	7.90	13.53	9.72
$^6Cu_5$	10.85	6.44	11.88	9.08
$^7Cu_6$	13.30	8.40	13.54	12.29
$^8Cu_7$	15.72	10.51	15.66	
$^9Cu_8$	16.09	10.75	15.23	
$^{10}Cu_9$	18.22	12.46	17.21	
$^{11}Cu_{10}$	19.00	13.18	18.14	
$^{12}Cu_{11}$	18.55	12.43	17.57	
$^{13}Cu_{12}$	18.90	12.66	17.93	
$^{15}Cu_{14}$	19.35	12.99	18.54	

difference is 1 kcal/mol (Table 3). Furthermore, the StuttgartECP-1997 data are as good as the ANO data and almost identical to the uncorrected LANDL2DZ data (Table 3). Therefore, the uncorrected LANL2DZ values are close to the "true" BDE/*n* values (ANO and StuttgartECP-1997 data); in contrast, the BSSE corrected LANL2DZ values are too low.

The geometries of the most stable no-pair clusters are presented in Figure 2 that exhibits two main trends. First, the clusters ($n = 2-12$) have high point group symmetries of $D_{\infty h}$ ($^3Cu_2$), D_{3h} ($^4Cu_3$), T_d ($^5Cu_4$), C_{4v} ($^6Cu_5$), C_{2v} ($^7Cu_6$), D_{5h} ($^8Cu_7$), C_{2v} ($^9Cu_8$), C_{3h} ($^{10}Cu_9$), D_{4d} ($^{11}Cu_{10}$), and C_2 ($^{12}Cu_{11}$; $^{13}Cu_{12}$). Generally, the most stable geometry for a given maximum-spin cluster is a compact structure with an optimal coordination number for each copper atom. Similar geometries and high symmetry and coordination numbers were obtained for $^{n+1}Li_n$ and $^{n+1}Na_n$ high-spin clusters. The second major trend is the variation of the total binding energy, expressed as the total bond dissociation energy (BDE; **values in boldface**) of the clusters. It is seen that the binding energy starts relatively small and then climbs steeply *in a manner that looks like nonadditive behavior*, which we have seen before for the $^{n+1}Li_n$ and $^{n+1}Na_n$ high-spin clusters. As shall be demonstrated this apparent nonadditive behavior can be understood using a VB model of bonding.

Figure 3 shows the evolution of bond dissociation energy per atom, BDE/*n*, as a function of the cluster size, *n*, for the $^{n+1}Cu_n$ clusters alongside the $^{n+1}Li_n$ and $^{n+1}Na_n$ clusters from previous work.[5,6] A few trends are projected from Figure 3. First, the BDE/*n* curves of the three clusters are quite similar; they are nonlinear in the cluster size and exhibit a few bumps and dips in the same cluster sizes, and cluster types, and the BDE/*n* quantity converges (to within less than 1 kcal mol^{-1}) around a cluster size of 10−14 atoms. Second, there are quantitative differences; the $^{n+1}Na_n$ clusters are only weakly bound with a maximum BDE/n = 3.5 kcal mol^{-1}, the $^{n+1}Li_n$ clusters are much more strongly bound, reaching BDE/*n* of 12 kcal mol^{-1}, but the $^{n+1}Cu_n$ clusters converge (to within 1 kcal mol^{-1}) at a much higher BDE/*n* value of 19 kcal mol^{-1}. This higher binding energy for the high-spin copper clusters was foreseen before by Bondybey, based on his comparison of the corresponding data for the dimers.[21]

4. Discussion

Clearly, the no-pair clusters exhibit a few interesting features, which have to be elucidated by an appropriate model. We need to understand the similar qualitative behavior of all the cluster types, the nonlinear rise of the BDE and BDE/*n* curves as a function of cluster size, the convergence of the BDE/*n* quantity, the tendency of the clusters for highly symmetric structures with large coordination numbers, and finally, the origins of such strong bonding in the absence of electron-pair bonds. The analysis will be based on the model presented in previous work on the alkali-metal clusters.[3,5]

4.1. Atomic Orbital Contributions to Bonding. Some preliminary and necessary insight can be gained by looking at the atomic orbital (AO) composition of the Kohn−Sham orbitals (KSOs) of the $^3\Sigma^+_u$ states in the no-pair dimers, $^3M_2$ (M = Li, Na, and Cu), in Figure 4. The bonding and antibonding, σ_{ns} and σ_{ns}*, combinations of the s-type valence AOs form the zeroth-order orbitals. These orbitals can then mix with other valence AOs, which possess the correct symmetry. The extent to which the latter orbitals mix into the zeroth-order orbitals is noted in Figure 4 by the weights of the corresponding orbitals.

In the cases of $^3Li_2$ and $^3Na_2$, in Figure 4a, the orbitals that can participate in mixing are the corresponding $2p_z$ and $3p_z$ AOs, respectively. As shown recently,[6] since the 2s−2p energy gap is smaller than the 3s−3p energy gap, the result is that the $^3Li_2$ dimer has a larger 2p contribution to the σ and σ* orbitals, compared with the 3p contribution in the $^3Na_2$ dimer; this is apparent by comparing the contributions of the *n*p AOs to the singly occupied orbitals of the Li and Na dimers in Figure 4a. In the case of $^3Cu_2$, in Figure 4b, in addition to the $4p_z$ orbital, there is substantial mixing of the filled $3d_{z^2}$ orbital. This latter mixing forms a 3-electron bonding interaction[34] that is generally stabilizing. These AO mixing patterns in the dimer are the key to the trends and dependence of BDE on the atomic identity in Figure 4. As the cluster grows, the weight of these higher angular momentum, AOs, in bonding increases, but the relative trends remain as in Figure 4 and carry over to the larger clusters. Thus, in the case of $^{n+1}Li_n$, there will be significant participation of 2p AOs in the FM-bonding of the cluster, while in $^{n+1}Na_n$ the 3p contribution will be much less significant, and finally, in $^{n+1}Cu_n$ there will be substantial 4p and 3d contributions to bonding.

4.2. A Valence Bond (VB) Model for FM-Bonding in $^{n+1}Cu_n$ Clusters. The $^3M_2$ Dimers. Figure 5a depicts the principal VB structures that were computed by means of ab initio VB theory using Hiberty's BOVB method,[35] and shown[3] to contribute to the FM-bonding in the no-pair dimer, $^3Li_2$. The fundamental structure, in which the electrons occupy the *2s* AOs of the two metal atoms, is denoted as $^3\Phi_{ss}$. As was demonstrated,[3] this structure by itself is always repulsive, and the bonding arises by mixing of a higher-lying covalent structure with electrons in $2p_z$ AOs of the two atoms, $^3\Phi_{zz}$(cov), and primarily of the ionic structures, $^3\Phi_{sz}$(ion), which arise by transferring an electron from the 2s orbitals of one Li to the $2p_z$ orbital of the other or vice versa. In the case of M = Na, we can use the same diagram as for M = Li just replacing 2s and 2p by 3s and 3p. However, as discussed in the preceding section, in the case of M = Cu, both 4p and 3d AOs participate in bonding, and therefore the number of VB structures is larger than in the alkali no-pair dimers. As shown in Figure 5a, now, there are two excited covalent and four ionic structures, which involve excitations from 4s to 4p and from 3d to 4s.

The VB calculations of $^3Li_2$ demonstrated[3] that the three excited structures, in Figure 5a, are quite high lying, and their mixing into the fundamental structure follows second-order perturbation theory. The corresponding VB mixing diagram for M = Li is shown in Figure 5b. The BDE of the FM-bond is seen to be a balance of the two terms; one is the repulsion energy, δE_{rep}, due to the triplet electrons in the 2s AOs, in the fundamental structure, the second is the stabilization energy due

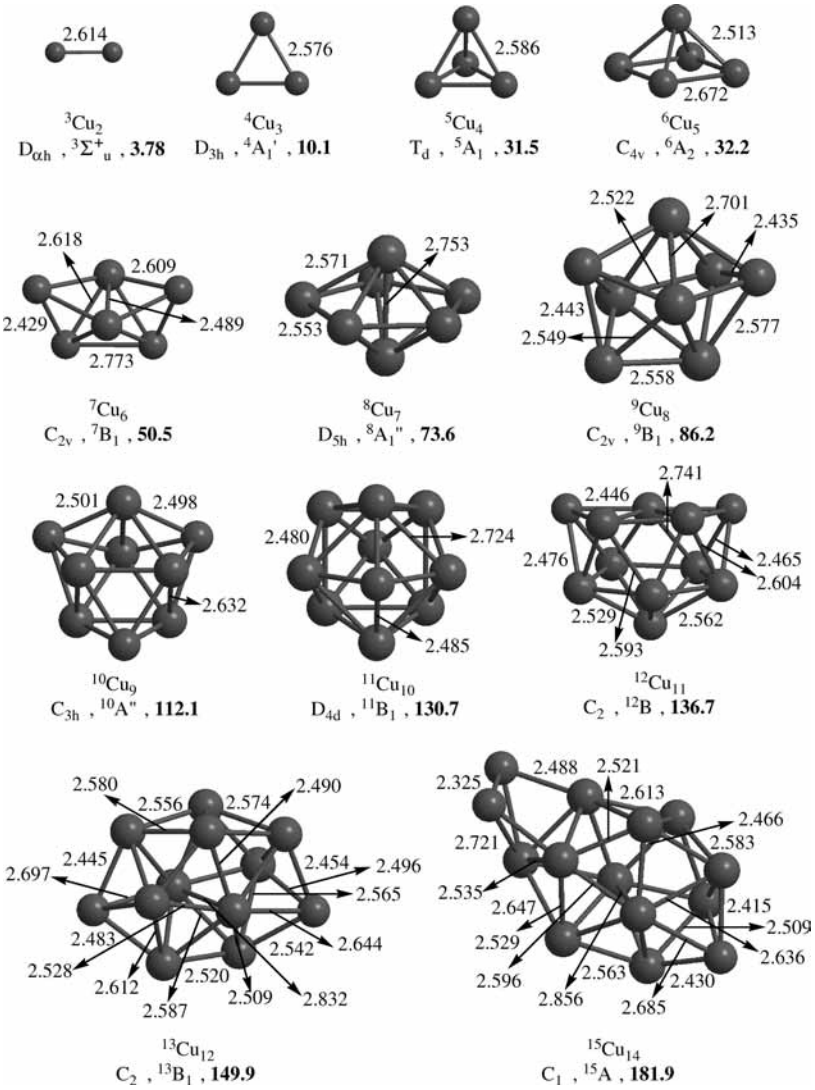

Figure 2. Structures of the most stable no-pair, $^{n+1}Cu_n$ ($n = 2-14$) clusters with symmetry, state assignment, and BDEs (UB3P86/LANL2DZ) relative to isolated atoms in kcal mol^{-1} (values in boldface with BSSE correction).

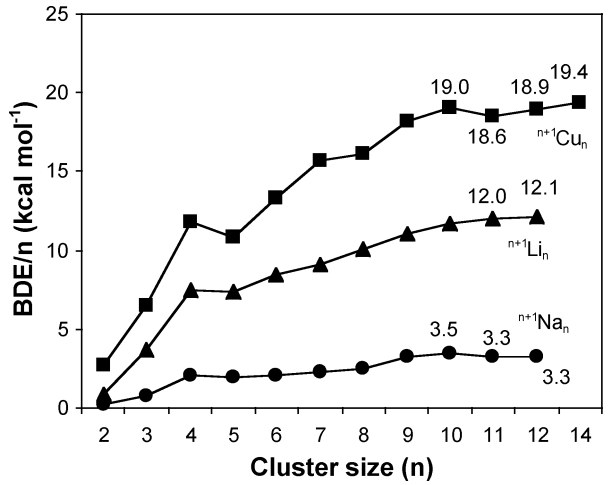

Figure 3. BDE/*n* trends for high-spin copper, lithium and sodium clusters. All calculations performed with Gaussian 98/Gaussian 03 using the UB3P86/LANL2DZ method. The trends for lithium and sodium were taken from refs 5 and 6.

to mixing, ΔE_{mix}, of the ionic and *zz*-covalent structures into the fundamental one. From the VB calculations,[3] the values are $\delta E_{rep} = 1.504$ kcal mol^{-1} and $\Delta E_{mix} = -2.19$ kcal mol^{-1}, leading a BDE value of 0.69 kcal mol^{-1}, in good accord with high level calculations such as CCSD(T) and CASPT2.[3] The VB calculations of $^3Na_2$ were done and show as expected a smaller BDE.[6] Unfortunately, VB calculations for $^3Cu_2$ cannot be done at the desired accuracy to derive reliable δE_{rep} and ΔE_{mix} quantities for this bond.[36]

Nevertheless, the VB model can be applied even in the absences of accurate calculations. As we mentioned already, the VB mixing follows perturbation theory,[3] and therefore, in principle, one only has to count the number of excited VB structures and consider their energy gaps relative to the fundamental structure, to reason qualitatively and semiquantitatively about the patterns of FM-bonding. Thus, the case of M = Na can simply be discussed using the diagram for M = Li in Figure 5b, but now the ionic and *zz*-covalent structures, which involve 3p AO occupancy, are higher lying compared with the fundamental structure, and hence the mixing will be smaller than in the case for M = Li. However, the case of M = Cu in Figure 5c is different, since now there are additional excited structures, involving the 3d → 4s excitations. As such, the total mixing term for M = Cu is likely to be greater than that for M = Li. Furthermore, since the repulsion term, δE_{rep}, due to the triplet 4s−4s electrons in $^3\Phi_{ss}$ of $^3Cu_2$, is not expected to be too different than the corresponding term for $^3Li_2$, the resulting BDE of the no-pair bond in $^3Cu_2$ will be significantly larger

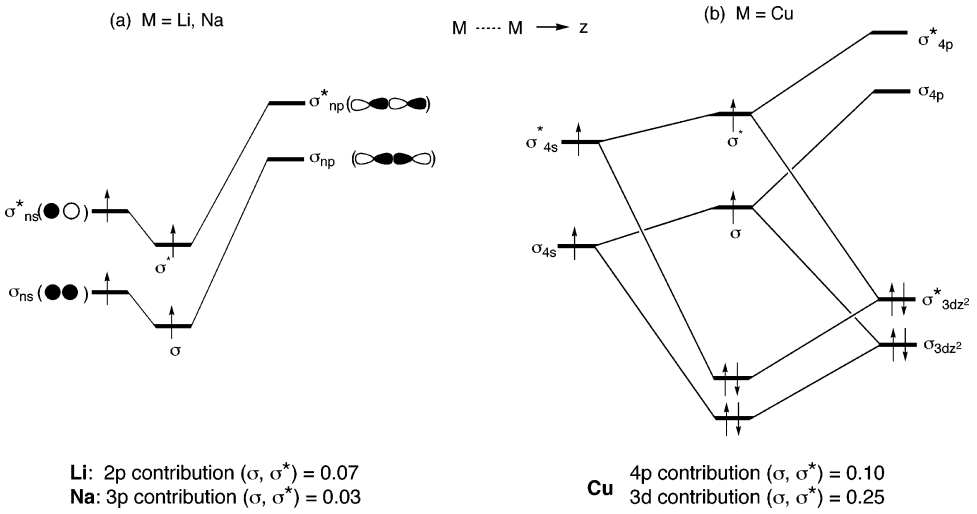

Figure 4. Mixing of n*p* and/or (*n*−1)d valence atomic orbitals (AOs) into the zeroth-order orbitals, σ_{ns} and σ_{ns}*, made from the bonding and antibonding combinations of the n*s* AOs. The σ and σ* are the final orbitals: (a) for $^3Li_2$ and $^3Na_2$ and (b) for $^3Cu_2$. In each case, the contribution of these valence AOs to the final orbitals is shown underneath the diagram.

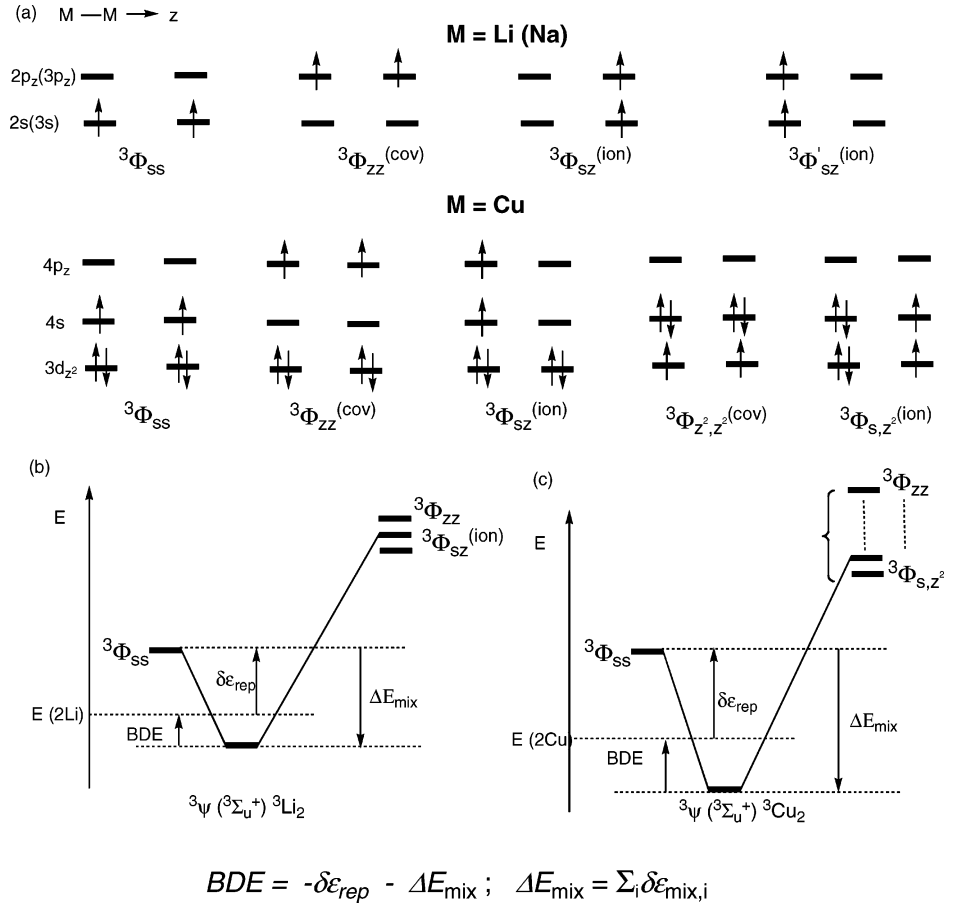

$$BDE = -\delta\varepsilon_{rep} - \Delta E_{mix}\ ;\quad \Delta E_{mix} = \Sigma_i \delta\varepsilon_{mix,i}$$

Figure 5. (a) Valence bond (VB) structures which contribute to ferromagnetic bonds in the no-pair dimers, $^3M_2(^3\Sigma^+_u)$, for M = Li and M = Cu; in the latter case we show only one of the two equivalent ionic structures for $^3\Phi_{sz}$(ion) and $^3\Phi_{sz^2}$(ion). (b & c) The corresponding VB mixing diagrams: (b) for M = Li and (c) for M = Cu. The expression for BDE is given in terms of the repulsion and mixing quantities.

than that for $^3Li_2$. This is indeed born out by the calculations and the experimental data regarding these no-pair dimers.[7−9,21] Another unique feature of $^3Cu_2$ is the 3-electron bonding interaction[34] endowed by the mixing of the excited structures, which involve excitation from the 3d orbitals.

The $^{n+1}M_n$ Clusters. In a cluster of size *n*, each atom will exchange electrons with the others atoms and give rise to many VB structures; however, the VB mixing diagram remains in principle the same as for the dimer and is schematized in Figure 6. The fundamental configuration is still the one with exclusive *n*s occupancy, namely the $^{n+1}\Phi_{s(1)\cdots s(i)\cdots s(n)}$ structure (in parentheses is the atomic index). This structure will mix with the multitude of excited VB structures, $^{n+1}\Phi_{ex}(i)$, $i = 1-N$, and will give rise to the FM-bonded no-pair $^{n+1}M_n$ cluster, with a BDE that scales with the number of excited configurations.

A simple model that was found useful for $^{n+1}Li_n$ clusters,[3,5] considers only those structures that arise from electron exchange (transfer, excitation) between close neighbor atoms, and neglects

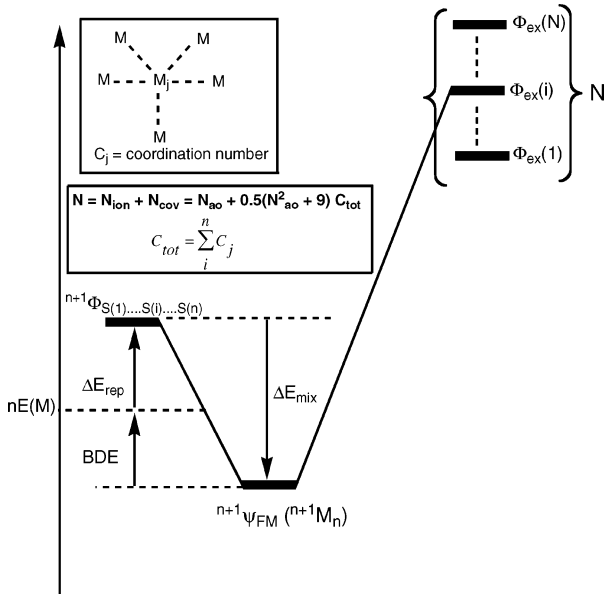

Figure 6. VB mixing diagram for a general no-pair cluster, $^{n+1}M_n$, of a mono-valent atom, M, with a coordination number C_j. The diagram shows the mixing of excited structures, $^{n+1}\Phi_{ex}(i)$, $i = 1-N$, into the fundamental structure, $^{n+1}\Phi_{s(1)\cdots s(i)\cdots s(n)}$. The number of excited structures with close neighbors electron exchange, for $^{n+1}Cu_n$, is given in the box; N_{ao} is the number of 4s and 4p AOs that participate, per atom, in the electron exchange (for 3d participation, see discussion later).

configurations with multiple excitations, retaining only singly ionic ones and excited covalent structures. In such a case, the number of excited VB structures depends on the coordination number of an atom, C_j, in the cluster and N_{ao}, the number of valence 4s and 4p AOs that participate in electronic exchange, and on the excitations from the filled 3d shell into these N_{ao} orbitals (see part B in the SI document). Moreover, since the mixing between the fundamental and its excited VB structures depends only on the close neighbor interactions,[3,5,37] this means that we can utilize the mixing energies extracted from the no-pair dimer and apply these quantities to the larger clusters.

The BDE expression, based on the mixing diagram and perturbation theory, is given in eq 1.

$$\mathrm{BDE} = -\Delta E_{rep} - \sum_i (\delta E_{mix,i}) \qquad (1)$$

Here, the first term is the repulsive interaction energy of all the pairwise close neighbor triplet pairs, within the fundamental structure, $^{n+1}\Phi_{s(1)\cdots s(i)\cdots s(n)}$, while the second term is the sum of all mixing terms due to the excited structures, indexed, $^{n+1}\Phi_{ex}(i)$. In part B of the SI document, we give detailed equations of the excited VB structure count using two different models (model I and model II), which differ on how one takes into account the doubly occupied orbitals (3d in case of $^{n+1}Cu_n$); here we follow with the main guidelines. The excited structures that we count maintain the total spin quantum number (maximum spin) of the fundamental structure, and involve three types, which follow the examples in Figure 4a: (i) the first is covalent structures, in which two electrons reside in two of the *n*p AOs of the atom and all other electrons reside in the *n*s orbitals, (ii) the second is singly ionic structures that arise from a single electron transfer from the *n*s AO of one atom to a *n*p AO of the other, and (iii) in the case of $^{n+1}Cu_n$, we allow also single electron excitations from a filled 3d AO to a 4s AO, etc. In the approach used in the following discussion (model II), we count only the transfers of β-electrons from 3d to 4s. In this manner, the 3d orbitals act as polarization functions for the 4s orbitals.

Using the simplifying assumption[3,5] that the various excited structures contribute identical mixing terms, δE_{mix}, eq 1 for the copper clusters becomes eq 2:

$$\mathrm{BDE} = -0.5C_{tot}\delta E_{rep} - [0.5(N_{ao}{}^2 + 9)C_{tot} + N_{ao}]\delta E_{mix}, \quad C_{tot} = \sum_j C_j \qquad (2)$$

where δE_{rep} is the close neighbor repulsive interaction, the variable N_{ao} is the number of singly occupied and virtual AOs (per atom) that participate in the electron exchange, while C_{tot} is the total coordination number summed over all atoms (j) in the clusters.

By comparison, the expression for the Li or Na clusters is given in eq 3, and the difference with eq 2 is due to the filled d-orbitals that contributed to the structure count in eq 2 and are absent in eq 3.

$$\mathrm{BDE} = -0.5C_{tot}\delta E_{rep} - [0.5(N_{ao}{}^2 - 1)C_{tot} + N_{ao}]\delta E_{mix} \qquad (3)$$

From our past experience with lithium and sodium no-pair clusters, the π-type interactions do not contribute significantly to FM-bonding.[3] Therefore, in a given cluster with a 3-dimensional shape, we used only the surface AOs, while the radial AOs were omitted from N_{ao}. Thus, for $^{n+1}Li_n$ clusters we have $N_{ao} = 3$, corresponding to the 2s AO and two out of the three 2p AOs. However, for Cu, the N_{ao} is not known to begin with, and will have to be determined by a best-fit procedure as outlined in the SI document.

Equations 2 and 3 can be used to estimate the total BDE of the cluster. The corresponding bond energies per atom, BDE/*n*, can be obtained by simply dividing by the number of the atoms in the cluster. One can further derive the value of BDE/*n* when $n \rightarrow \infty$, assuming that in eqs 2 and 3, all coordination numbers are identical and equal to some C, where $C = C_{tot}/n$, thus leading to

$$\mathrm{BDE}/n = -0.5C\delta E_{rep} - 0.5(N_{ao}{}^2 + 9)C\delta E_{mix}; \quad n \rightarrow \infty, \text{ for } {}^{n+1}Cu_n \qquad (4a)$$

$$\mathrm{BDE}/n = -0.5C\delta E_{rep} - 0.5(N_{ao}{}^2 - 1)C\delta E_{mix}; \quad n \rightarrow \infty, \text{ for } {}^{n+1}Li_n \qquad (4b)$$

Thus, assuming that in an infinite cluster the uniform coordination number is $C = 5$, we can estimate the convergence of the BDE/*n* quantity for a cluster of infinite size. Equations 2−4 show that, because of the rapid increase in the mixing energy terms, due to the interaction possibilities per atom, the FM-binding energy of the no-pair cluster will behave in a nonadditive manner with the growth in the number of atoms in the cluster.

Figure 7 shows the reproduced data calculated[5] with eq 3, using the VB values of δE_{rep} (1.504 kcal mol^{-1}) and δE_{mix} ($\delta E_{mix} = 1/3\Delta E_{mix} = -0.73$ kcal mol^{-1}) for the $^3Li_2$ no-pair dimer, where $N_{ao} = 3$ (recall that the value of N_{ao} neglects the 2p orbital that are radial to the surface of the cluster due to weak π-type interactions[3,5]). The so estimated data is plotted alongside the data computed by means of the UB3P86 functional. The fit of the model curve to the UB3P86 computed one is seen to be reasonably good. It reproduces the initial fast rise of the BDE/*n*, the convergence of this quantity for cluster size of $n = 10-12$, and the tendency of the cluster to assume compact structures with optimal coordination number. Furthermore, the converged BDE/*n* for *n*-infinite based on eq 4b is

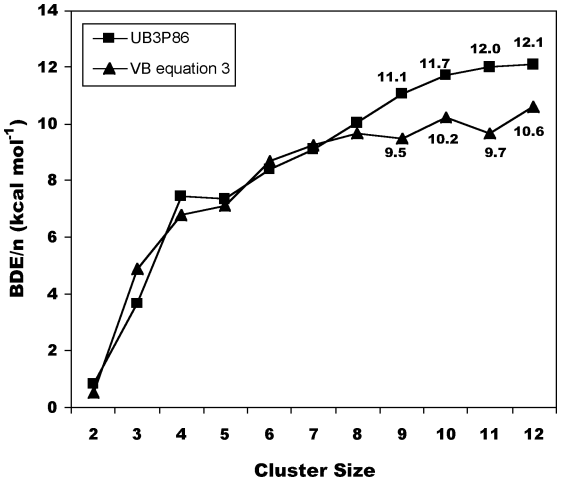

Figure 7. Plots of BDE/*n* for $^{n+1}Li_n$ no-pair clusters vs the cluster size, *n*. One curve is calculated with the model VB equation (eq 3), the other with the UB3P86 functional. The plot is reproduced from ref 6 with permission of the ACS.

10.8 kcal mol^{-1}, while the converged B3P86 value is approximately 12 kcal mol^{-1}. The model explains another important trend, the propensity of the no-pair clusters to form symmetric structures. This tendency is controlled by the repulsive term in eq 3, $0.5C_{tot}\delta E_{rep}$. Mathematically, this term is minimized when all the distances for a given atom in the cluster are equal to one another. This would therefore act as a driving force to symmetrize the clusters, as much as possible, to reduce the repulsive energy. At the same time, the mixing term, which is a collection of individual terms, would be maximized for symmetric structures (per a given total bond length).

Let us now apply the same model to the no-pair clusters of Copper. In this case, we lack VB values for the terms, δE_{rep} and δE_{mix}, which are needed for calculating the BDE and BDE/*n* from eq 2 in a direct manner. However, we can still apply the equation by finding the best-fit parameters. The fit was obtained by assuming that the repulsive term, δE_{rep}, for $^{n+1}Cu_n$ is the same as in the corresponding $^{n+1}Li_n$ clusters, and then finding the least-squares fit for δE_{mix} using various reasonable values for N_{ao}; the approach is detailed in the SI document (part B). Many fits were tried (Tables S.I and S.II in the SI document) and led to results of rather similar quality. There is a trade off between the number of VB structures and the value of the fitted δE_{mix} parameter; the larger the number of structures, the smaller the value of δE_{mix}, and vice versa. Here, in Figure 8, we show the most reasonable fit, for which $N_{ao} = 3$, the same as in the Li_n cluster, and in addition all the occupied 3d orbitals are allowed to transfer single electrons to the 4s orbitals. For this fit we obtain a δE_{mix} value of -0.49 kcal/mol, and convergence of the BDE/*n* values to 18$-$19 kcal mol^{-1}.

The fit between the estimated and UB3P86 computed data, while not perfect, is still reasonable since it reproduces the global behavior of the BDE/*n* quantity, in terms of its rise and convergence (within 1 kcal mol^{-1}). It is seen that the LANL2DZ and Stuttgart/ECP-1997 give similar fits. Furthermore, using eq 4a, we can derive the converged bond dissociation energy per atom as, BDE/*n* ($n \rightarrow \infty$) = 18.3 kcal mol^{-1}, compared with the UB3P86 computed datum of 19$-$19.3 kcal mol^{-1}. Finally, Figure 9 shows a linear regression plot of the estimated vs the UB3P86/LANL2DZ computed BDE/*n* data. The correlation coefficient of 0.976 is fairly good considering the crudeness of the model. The same quality of correlation and fit were obtained using the BSSE corrected BDE/*n* values (Tables S.1b and S.IIb), which as we showed (Table 3, Figure 1) exhibit the same trends as the "true" values, but are lower.

Thus, Figures 8 and 9 show that the VB model captures the essence of FM-bonding in no-pair clusters. The model shows that a weak interaction in the dimer can become a remarkably strong binding force that binds together mono-valent atoms without even a single electron pair. This is achieved because the steeply growing number of VB structures exerts a cumulative effect of stabilization that is maximized when the cluster is compact with an optimal coordination number of the atoms. Thus, *the nonadditive behavior of the binding energy is scaled by the number of VB structures available for mixing with the fundamental repulsive structure*, $^{n+1}\Phi_{s(1)\cdots s(i)\cdots s(n)}$.

The best way to conceptualize no-pair bonding is as an ionic fluctuation of the triplet pairs that spread over all the close neighbors of a given atom in the clusters. Thus, if we consider each diatomic triplet pair and its ionic (covalent) fluctuations as a local FM-bond, we can regard the electronic structure of a given $^{n+1}M_n$ cluster as *a resonance hybrid of all the local FM-bonds between close neighbors*. In the case of Li, the local FM-bond involves only two electrons in $N_{ao} = 3$ orbitals, while in the Cu clusters, there is an additional and a strong component of 3-electron bonding due to the participation of the filled 3d-orbitals in the ionic fluctuation. This VB model bears relationship to the GBV model of McAdon and Goddard[1] who discussed no-pair bonding of Li_n rings in terms of resonance hybrids with interstitial orbitals. It would be interesting to see other representations of FM-bonding, e.g., by means of electron localization

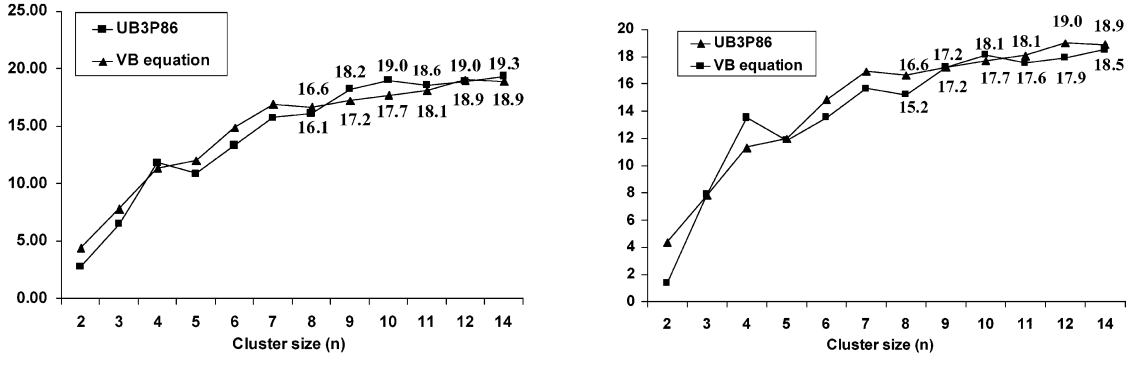

(a) BDE/n, UB3P86/LANL2DZ data (b) BDE/n, UB3P86/StuttgartECP-97 data

Figure 8. Plots of BDE/*n* for $^{n+1}Cu_n$ no-pair clusters vs the cluster size, *n*. The curve with the triangular data points, is calculated with the model VB equation (eq 2) for $N_{ao} = 3$, $\delta E_{mix} = -0.49$ kcal mol^{-1}, and $\delta E_{rep} = 1.504$ kcal mol^{-1}. The other curve, with the square data points, corresponds to the UB3P86 calculated values. Key: (a) LANL2DZ data; (b) Stuttgart/ECP-1997 data.

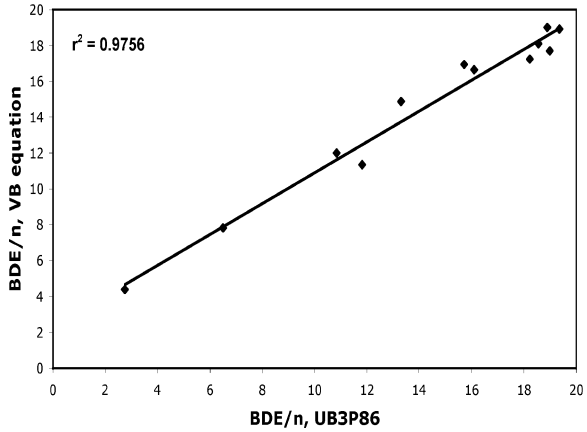

Figure 9. Linear regression plot of the BDE/*n* data for $^{n+1}Cu_n$ calculated with eq 2 against the data calculated with the UB3P86/LANL2DZ functional.

function (ELF)[38] calculations or other electron density-based methods (e.g., atoms in molecules, AIM).[39,40]

5. Conclusions and Summary

We studied in this paper high-spin copper clusters $^{n+1}Cu_n$ ($n = 2-14$), which are devoid of electron pairs, and found the bond dissociation energy per atom to converge at around 10−14 atoms in the cluster with a BDE/$n \sim 18-19$ kcal mol^{-1}. This is much larger than obtained for lithium clusters (12 kcal mol^{-1}) or sodium clusters (3 kcal mol^{-1}).

The remarkable finding here is how by the sheer cumulative effect of the interaction possibilities of an atom in a cluster, a weak interaction in the dimer becomes a strong robust interaction in a cluster of size 10−14. Thus, a weak local FM-bond in the dimer creates strongly bound no-pair clusters, with a bond energy of 19 kcal·mol^{-1} per atom, and with high magneticity. Chemistry will have to reckon with no-pair FM-bonding as a building block in the philosophical construct we call "chemical bonding".

Acknowledgment. The research was supported by an ISF grant to S.S.

Note Added after ASAP Publication. This article was published ASAP on April 7, 2006. The caption of Figure 2 has been corrected. The correct version was reposted on April 13, 2006.

Supporting Information Available: Text giving the full ref 22, tables of Cartesian coordinates, tables giving details of the BDE fit, tables giving the connectivity matrix, a figure showing the localized orbitals, text giving VB model equations, and tables showing the results of the fits. This material is available free of charge via the Internet at http://pubs.acs.org.

References and Notes

(1) McAdon, M. H.; Goddard, W. A., III. *J. Phys. Chem.* **1988**, *92*, 1352.

(2) Glukhovtsev, M. N.; Schleyer, P. v. R. *Isr. J. Chem.* **1993**, *33*, 455.

(3) Danovich, D.; Wu, W.; Shaik, S. *J. Am. Chem. Soc.* **1999**, *121*, 3165.

(4) de Visser, S. P.; Alpert, Y.; Danovich, D.; Shaik, S. *J. Phys. Chem. A* **2000**, *104*, 11223.

(5) de Visser, S. P.; Danovich, D.; Wu, W.; Shaik, S. *J. Phys. Chem. A* **2002**, *106*, 4961.

(6) de Visser, S. P.; Danovich, D.; Shaik, S. *Phys. Chem. Chem. Phys.* **2003**, *5*, 158.

(7) Higgins, J.; Hollebeek, T.; Reho, J.; Ho, T.-S.; Lehmann, K. K.; Rabitz, H.; Scoles, G.; Gutowski, M. *J. Chem. Phys.* **2000**, *112*, 5751.

(8) Brühl, F. R.; Miron, R. A.; Ernst, W. E. *J. Chem. Phys.* **2001**, *115*, 10275.

(9) Fioretti, A.; Comparat, D.; Crubellier, A.; Dulieu, O.; Masnou-Seeuws, F.; Pillet, P. *Phys. Rev. Lett.* **1998**, *80*, 4402.

(10) For a few of the earlier calculations of these bound dimers, see: (a) Kutzelnigg, W.; Staemler, V.; Gélus, M. *Chem. Phys. Lett.* **1972**, *13*, 496. (b) Olson, M. L.; Konowalow, D. D. *Chem. Phys.* **1977**, *21*, 393. (c) Konowalow, D. D.; Olson, M. L. *Chem. Phys.* **1984**, *84*, 462.

(11) It should be noted that the mixing of these structures is not equivalent to a simple $2s-2p_z$ hybridization effect, as evidenced by the fact that the Hartree−Fock (HF) wave function for $^3Li_2(^3\Sigma^+_u)$, is unbound and repulsive throughout the internuclear distance,[3] despited the significant hybridization of the 2s and $2p_z$ orbitals, more so than in the post HF wave functions.

(12) Higgins, J.; Callegari, C.; Reho, J.; Stienkemeier, F.; Ernst, W. E.; Lehmann, K. K.; Gutowski, M.; Scoles, G. *Science* **1996**, *273*, 629.

(13) Higgins, J.; Ernst, W. E.; Callegari, C.; Reho, J.; Lehmann, K. K.; Scoles, G. *Phys. Rev. Lett.* **1996**, *77*, 4532.

(14) Higgins, J.; Callegari, C.; Reho, J.; Stienkemeier, F.; Ernst, W. E.; Gutowski, M.; Scoles, G. *J. Phys. Chem. A* **1998**, *102*, 4952.

(15) Reho, J. H.; Higgins, J.; Nooijen, M.; Lehmann, K. K.; Scoles, G.; Gutowski, M. *J. Chem. Phys.* **2001**, *115*, 10265.

(16) (a) Cvitas, M. T.; Soldan, P.; Huston, J. M. *Phys. Rev. Lett.* **2005**, *94*, 033201. (b) Quemener, G.; Honvault, P.; Launay, J.-M.; Soldan, P.; Potter, D. E.; Houston, J. M. *Phys. Rev. A* **2005**, *71*, 032722.

(17) Cvitas, M. T.; Soldan, P.; Houston, J. M.; Honvault, P.; Launay, J.-M. *Phys. Rev. Lett.* **2005**, *94*, 200402.

(18) McAdon, M. H.; Goddard, W. A., III. *J. Chem. Phys.* **1988**, *88*, 277.

(19) Morse, M. D. *Chem. Rev.* **1986**, *86*, 1049.

(20) Lombardi, J. R.; David, B. *Chem. Rev.* **2002**, *102*, 2431.

(21) Bondybey, V. E. *J. Chem. Phys.* **1982**, *77*, 3771.

(22) (a) Frisch, M. J.; et al. *Gaussian-98*; Pittsburgh, PA, 1998. (b) Frisch, M. J.; et al. *Gaussian-03*; Wallingford, CT, 2004.

(23) (a) Becke, A. D. *J. Chem. Phys.* **1992**, *96*, 2155. (b) Becke, A. D. *J. Chem. Phys.* **1992**, *97*, 9173. (c) Becke, A. D. *J. Chem. Phys.* **1993**, *98*, 5648.

(24) Lee, C.; Yang, W.; Parr, R. G. *Phys. Rev. B* **1988**, *37*, 785.

(25) Perdew, J. P. *Phys. Rev. B* **1986**, *33*, 8822.

(26) Perdew, J. P.; Wang, Y. *Phys. Rev. B* **1992**, *45*, 13244.

(27) (a) Hay, J. P.; Wadt, W. R. *J. Chem. Phys.* **1985**, *82*, 299. (b) Friesner, R. A.; Murphy, R. B.; Beachy, M. D.; Ringlanda, M. N.; Pollard, W. T.; Dunietz, B. D.; Cao, Y. X. *J. Phys. Chem. A* **1999**, *103*, 1913.

(28) Dolg, M.; Stoll, H.; Preuss, H.; Pitzer, R. M. *J. Phys. Chem.* **1993**, *97*, 5852.

(29) Schafer, A.; Horn, H.; Ahlrichs, R. *J. Chem. Phys.* **1992**, *97*, 2571.

(30) (a) Wachters, A. J. H. *J. Chem. Phys.* **1970**, *52*, 1033. (b) Bauschlicher, C. W., Jr.; Langhoff, S. R.; Partridge, H.; Barnes, L. A. *J. Chem. Phys.* **1989**, *91*, 2399.

(31) Pou-Amerigo, R.; Merchan, M.; Nebot-Gil, I.; Widmark, P. O.; Roos, B. *Theor. Chim. Acta* **1995**, *92*, 149.

(32) All basis sets that are not presented in Gaussian-03 package were taken from following location: http://www.emsk.pnl.gov/forms/basisform-.html.

(33) Wang, X.; Wan, X.; Zhou, H.; Takami, S.; Kubo, M.; Miyamoto, A. *THEOCHEM* **2002**, *579*, 221.

(34) (a) Hiberty, P. C.; Humbel, S.; Archirel, P. *J. Phys. Chem.* **1994**, *98*, 11697. (b) Braïda, B.; Thogersen, L.; Wu, W.; Hiberty, P. C. *J. Am. Chem. Soc.* **2002**, *124*, 11781.

(35) (a) Hiberty, P. C.; Flament, J. P.; Noizet, E. *Chem. Phys. Lett.* **1992**, *189*, 259. (b) Hiberty, P. C. In *Modern Electronic Structure Theory and Applications in Organic Chemistry*; Davidson, E. R., Ed.; World Scientific: River Edge, NJ, 1997; pp 289−367.

(36) For particular difficulties to compute $Cu-H^+$ using VB theory, see: Galbraith, J. M.; Shurki, A.; Shaik, S. *J. Phys. Chem. A* **2000**, *104*, 1262.

(37) Shaik, S. S. A Qualitative Valence Bond Model for Organic Reactions. In *New Theoretical Concepts for Understanding Organic Reactions*; Bertran, J., Csizmadia, I. G., Eds.; NATO ASI Series C267; Kluwer Academic Publ.: Dordrecht, The Netherlands, 1989; p 165.

(38) (a) Silvi, B.; Sevin, A. *Nature* **1994**, *371*, 683. (b) Savin, A. *J. Mol. Struct: THEOCHEM* **2005**, *2005*, 127.

(39) Bader, R. F. W.; Nguyen-Dang, T. T. *Adv. Quantum Chem.* **1981**, *14*, 63.

(40) Kraka, E.; Cremer, D. In *Theoretical Models of Chemical Bonding*; Maksic, Z. B.; Ed.; Springer-Verlag: New York, Part 2, pp 457−543.